Investigating the opacity of a Delta Scuti variable star and a new stellar model based on empirical results

2663452

April 14, 2024

Abstract

In this paper the ability to determine the change in opacity of a single star is investigated by use of light curves and the determination of temperature from colour, and how this could be expanded for a cluster of stars of a similar type to construct a new stellar model based on the empirical internal structure of a short period, intrinsic variable star.

1 Introduction and Background

Intrinsic variable stars are post main sequence stars that due to their composition exhibit a variation in their apparent magnitudes. They appear on the Hertzsprung-Russell Diagram on the instability strip this can be seen in Figure 1, which is a section just off the main sequence that stars can evolve onto, it has some discrete sections for each type of variable (δ Scuti stars are closer to the MS than most with a lower luminosity than there Cepheid counter parts).

For the last 100+ years intrinsic variable stars have been a prominent field of research as astronomers hope to understand the full cycle of a stars lifetime. They can be classified based on the length of their period of variation, their composition (metallicity content) and the magnitude of their variation [2]. The group that is of interest in this report is commonly referred to as HADS or High amplitude delta scuti (δ scuti) these stars typically have periods of around 0.05 - 0.3 days [3] and amplitude variations of above 0.1 magnitudes [2] in the V Band (V Johnson filter system [4]).

1.1 Intrinsic Variation

The variation in the magnitude of δ Scuti stars is a result of unbalanced forces within the stars interior, the star is assumed to not be in hydrostatic equilibrium. If the star is at its brightest then the star is fully expanded and has its greatest radius, at this point the convection layer near the exterior of the star has become less opaque allowing for radiation to escape and gravitational pressure dominates causing the star to contract, thus increasing the temperature and increasing ionisation, which by free-free absorption increases the opacity, allowing less radiation to escape and increasing

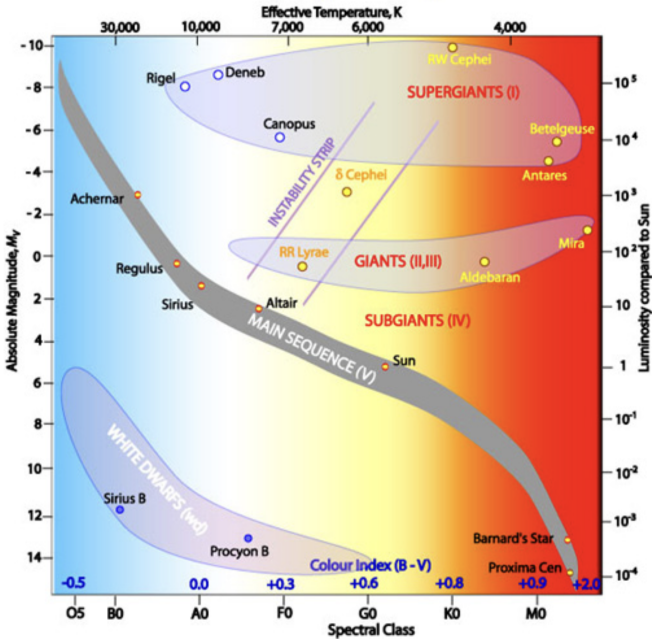

Figure 1: Hertzsprung-Russell diagram showing the different stages of evolution of star and the instability strip (upper middle) where post main sequence variable stars are located [1].

the radiation pressure until it overcomes gravity, at which point the star expands. This oscillation continues, with only a small amount of energy lost due to kinetic friction between convection zones acting as a damping factor. For converting from colour to temperature equation (1) will be used as derived from the Sloan Digital Sky Survey (SDSS) data [5].

$$T_{\text{eff}} = \frac{1.09}{g' - r' + 1.47} \times 10000\,\text{K} \tag{1}$$

1.2 The Kappa Mechanism

As mentioned the opacity of a star is linked to its temperature in the convection zone, this is due to the type of ionisation of the gas at certain temperatures. For example at high temperatures the gas can be considered to be fully ionised this results in a gas of free electrons and ions, thus when photons interact with these electrons it is free-free absorption, and at lower temperatures the gas may be only partially ionised and bound-free or even bound-bound absorption takes place. The opacity for temperatures greater than $2{\times}10^4$ K and less than $1{\times}10^7$ K [6, 7] can be given by κ_{ff} the Kramer's opacity for free-free absorption which is

$$\kappa_{ff} = \kappa_{0,ff}\rho T^{-3.5} \tag{2}$$

where ρ is the density of the star T is the Temperature and $\kappa_{0,ff}$ is a coefficient based on the atomic composition of the gas. This opacity has been used as an approximation here as it is not possible to calculate the opacity from the data received therefore only showing a proportionality relationship.

1.3 The Ability to Construct a New Stellar Model

In order to construct a stellar model more information is needed about the target star, such as the distance to the star, the luminosity and then from this the radius and mass for target variable stars. This can be achieved with the use of parralax (if observations can be done 6 months apart), or by use of constructing a period luminosity relationship for a Cepheid or RR Lyrae type variable star to determine distance [8]. Then using equation (2) to find the opacity and using knowledge of expansion and contraction of gases, as well as Lomb scargle periodogram to accurately determine the period of oscillation within the star, a full radial model may be created for either a single star or an entire cluster that share similar properties [9].

2 Optical Astronomy

A key component of this project was the ability to understand and complete accurate astronomical observations and calibration with use of the remote telescope in Almeria, Spain as supplied by Mr. P. Kent. To do so it was necessary to locate suitable variable stars that would be visible longer than their period during the night (this required them to be above 30° azimuth and to not pass through the zenith of the telescope), there were a few ways to go about this but by far the most effective was the use of Vizier [10] (a published library of astronomical data) and to search for a catalogue of interest (for example "Mono-periodic pulsating stars in the OGLE database (Poretti, 2001) [11]", which contains many δ Scuti stars), from here stars that fit roughly the correct Right Ascension (RA), Declination (DEC) and period requirements could be located using a online planetarium software, (such as Stellarium [12] or Aladin Sky Atlas [13]) this allows the ability to check the star will be visible to the telescope for long enough in the night. Once suitable stars had been selected the celestial coordinates (RA and DEC) were given to the telescope operator and exposure times were decided based on the expected magnitude of the star as to not saturate the CMOS sensor.

2.1 The Sloan Filter System

The telescope is equipped with the g', r' and i' filters from the Sloan photometric filter system [14] and a CMOS active pixel sensor, all observations were done in at least 2 of the three filters as this allows for the computation of colour (the third filter is emitted in long exposure observations to allow for a quick enough return time to the initial filter allowing for higher sampled light curves).

2.2 Calibration Frames

When using CMOS sensors for optical astronomy it is important to remove the noise received by the sensor during imaging. This comes in a few forms, first there are so called hot pixels, these are a result of excess currents flowing through the drain of the transistors that supply the read-out signal for each pixel, these are permanent and can be removed by taking a Dark frame (which is a frame with the same exposure length as the image, but with the lens cap on and in a dark environment). The next

is the Flat frames these are taken for each filter with the lens cap on and a bright light in front of the telescope to give even illumination of the sensor, these frames help remove any vignetting or dust present on the telescope. Finally are the Bias frames which act as a Dark frame for calibrating the Flat frames removing any potential hot pixels in the flat frame (these were all supplied by the telescope operator with the suitable exposure times and temperatures).

3 Calibration and Plate solving

Once the data was received it was necessary to calibrate it using the Dark, Flat and Bias frames as described above the correct way to do this is shown in (3)

$$\frac{\text{Science} - \text{Dark}}{\text{Flat} - \text{Bias}} \times (\overline{\text{Flat} - \text{Bias}}) \tag{3}$$

where Science is the data frame and $\overline{\text{Flat} - \text{Bias}}$ is the average pixel value of Flat − Bias.

These calibrated images now have less noise making the flux per pixel more accurate to the object being observed. From here a process called platesolving was used, in which the images and a list of the sources (a source is any object in the image with a higher brightness than the background of the image, the definition of a source can be changed by adjusting how much brighter it must be compared to the background), present in the image are uploaded to a server that compares the images and sources in them to patches of the night sky with known sources in the same pattern.

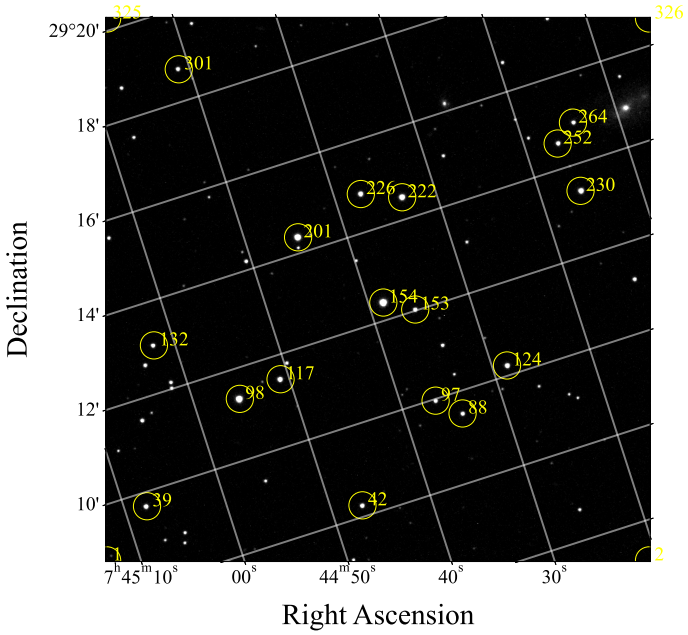

Figure 2: Platesolved image in RA and DEC with the target star NSVS7293918 at position 154

The server used here is provided by Astrometry.net [15]. This returns the image and the RA and DEC of the sources within the image this new image can be seen in

Figure 2 the RA and DEC are then embedded into the image header as they will be required for the next stages of processing.

4 Photometry

4.1 Aperture Photometry

Before obtaining light curves its necessary to calibrate the aperture of the target star (the aperture is a circle around the target that contains all the flux of the target), this will require the aperture to be set right at the edge, this can be by use of a curve of growth which shows the amount of flux in a radius r this can be seen in Figure 3 from this graph the ideal radius is the one that minimises the gradient below a set threshold, this can be seen to be approximately r = 9 for the g' band of NSVS7292918.

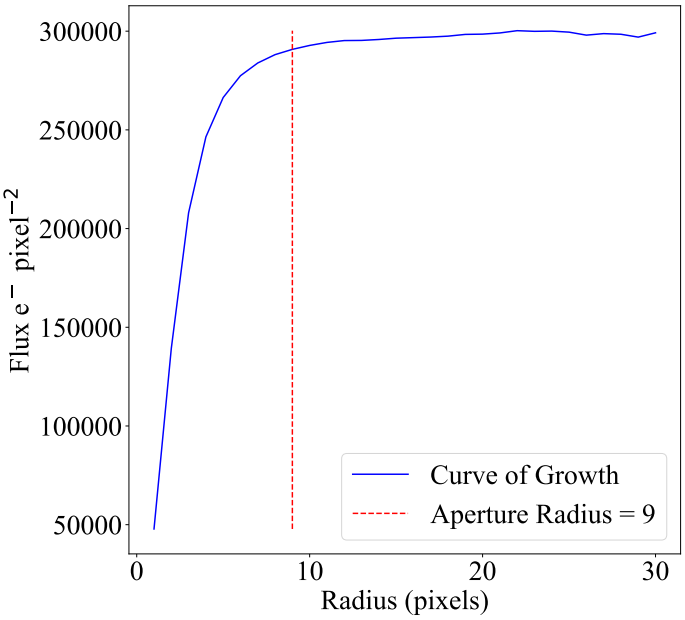

Figure 3: Curve of growth for NSVS7293918 showing the amount of flux received per aperture size, with the chosen aperture of nine plotted.

To calibrate the aperture an average flux of the background of the image is required in units Flux pix^{-2} which can be found by creating an annulus around the target and dividing the flux in this region by the area. This is then taken away from the aperture area giving a new flux that is entirely due to the radiation emitted by the star. The magnitude of the target star can be calculated via differential photometry or by the use of the zero point of the calibration stars and a calculation of the extinction due to atmospheric reddening and the air mass (4)

$$X = \sec(\mathrm{z}) \tag{4}$$

where X is the air mass and z is 90 minus the altitude. In this report differential photometry was used as a rough check for light curves then zero point calculations were done as well as extinction to obtain final values for apparent magnitude.

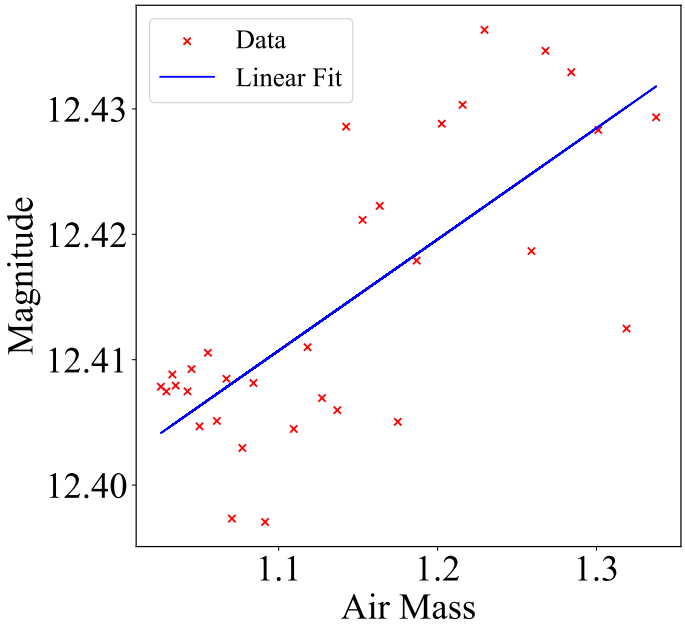

Figure 4: Magnitude as a function of distance for a calibration star, the gradient of the line is the extinction coefficient and is, $0.08869 \pm 0.01472\,\mathrm{km}^{-1}$

4.2 Calculating Magnitude via the Zero Point

The zero point can be calculated using equation (5) [16, 17]

$$m_{\mathrm{zp}} = m_{\mathrm{cal},i} - kX \tag{5}$$

where $m_{\mathrm{cal},i}$ is the instrumental magnitude of a calibration star calculated by equation (6) [16, 17], X is the air mass and k is the extinction coefficient (calculated by plotting the instrumental magnitude against the air mass as a function of angle, the gradient of this line is then the extinction coefficient, an example can be seen in Figure 4

$$m_i = -2.5 \log f \tag{6}$$

where m_i is the instrumental magnitude, and f is the flux received for a particular star. And finally using equation (7) [16, 17] it is possible to calculate the above atmosphere corrected magnitude.

$$m_{\mathrm{app}} = m_i + m_{\mathrm{zp}} - kX \tag{7}$$

This process is initially completed for non-variable calibration stars near to the target star and once the zero point and extinction coefficient has been accurately deduced the target star can be calibrated for each image, the apparent magnitude of the target is then plotted against Julian Date and the result for the g' and r' bands for NSVS7293918 can be seen in Figure 5.

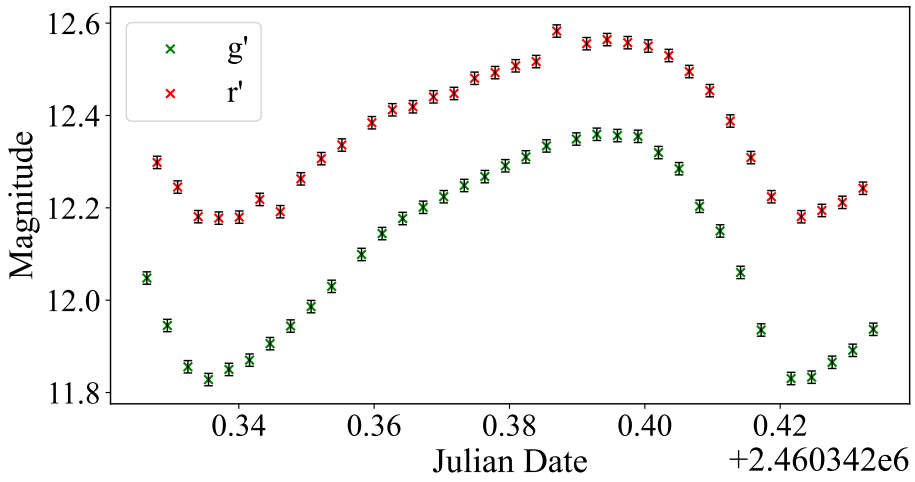

Figure 5: Magnitude against Julian Date for the g' and r' bands of NSVS7292918, showing a distinct light curve with approximately 0.4 magnitudes of change per band.

5 Determining the Temperature Throughout the Period

5.1 Stellar Colour of NSVS7293918

As NSVS7293918 was observed in multiple filters we are able to calculate the stellar colour of the star (Stellar colour is related to a stars surface temperature and spectral type, closely linking it to a position on the Hertzsprung-Russell diagram as seen in Figure 1) The colour is calculated by taking g'−r' and a plot of the colour (with associated errors propagated from the magnitudes) over time can be seen in Figure 6.

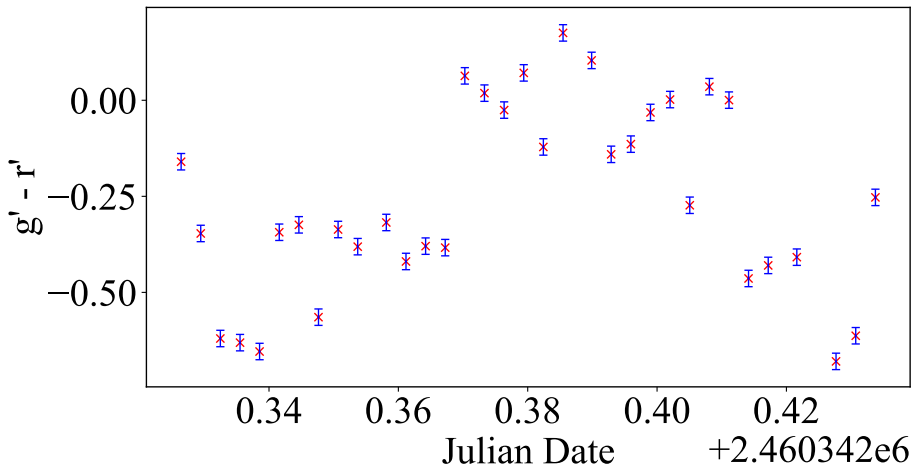

Figure 6: g' − r' colour of NSVS7293918 over time

Figure 6 shows that during the course of the night the colour within the star changes by over 0.5 magnitudes, this can be related to temperature as more of the photons received are towards one side of the optical spectrum, this is associated with

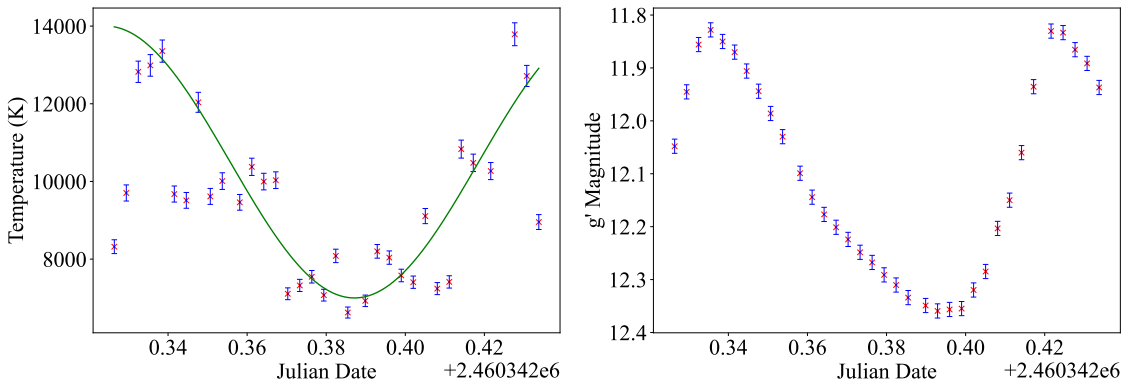

Figure 7: Left: Temperature over time fitted with an approximated sinusoidal line of best fit, Right: the g' band magnitude over time, this shows for a decreasing magnitude value the temperature of the star decreases.

an energy change and thus the temperature of the gas that emits photons.

5.2 Temperature Relationship

By using equation (1) the temperature at each of these stages can be calculated and plotted as a time series over the duration of a night. When comparing this to the magnitude time series there is a clear correlation between the brightness of a star and its effective temperature, where there is a decrease in brightness there is a significant decrease in the temperature, this can be seen in Figure 7 where the magnitude y axis is inverted due to a lower value corresponding to an increase in magnitude.

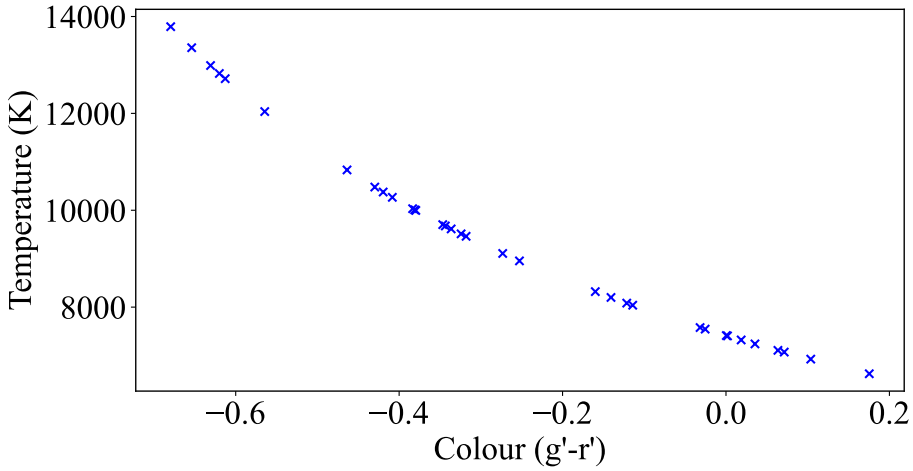

Figure 8: Effective temperature of NSVS7293918 against its colour showing for lower temperatures stars appear more red.

This relationship between temperature can be more accurately seen through the use of a temperature colour plot as seen in Figure 8, as color is directly proportional to the magnitude, and temperature and colour are inversely related the resultant plot is expected to be a downwards trend, this shows that for young stars, those typically

of lower temperature the colour will be a larger number as more photons are being emitted in the red band.

6 Opacity and Stellar Pulsations

As outlined in the introduction using equation (2) the opacity κ is directly proportional to the effective temperature with a varying density ρ and a constant of proportionality of κ_0 which is dependent on the fraction of Hydrogen, Helium and metals within the star.

Due to limitations of the lab and the inability to calculate the mass and radius of the star in a compressed time limit, a distinct value for opacity has not been calculated. As the temperature has been shown to vary in Figure 7 it is possible to deduce that the opacity in the convection zone of the star must change with temperature as the radius can only undergo small finite changes, as temperature within the star increases the energy from an increase in temperature initially is used to increase the ionisation of the gas, before undergoing expansion due to the ideal gas law (8) at constant pressure. This leads to the observed stellar pulsations within the star.

$$PV = nRT \tag{8}$$

6.1 A New Stellar Model

Models for variable stars are inherently difficult due to the number of parameters required for each stage as well as the assumption that a star cannot be in hydrostatic equilibrium. For a single star an accurate model would be extremely difficult as the period may change over the observation lifetime as the internal properties change, however, for a cluster of stars it may be easier. Clusters of stars have been shown to have similar stellar properties such as age, temperature and composition [18, 19], allowing for the computation of the required parameters by using the non variable companions that are present in a cluster.

6.2 A Potential Cluster Candidate

As was identified during the search for variable stars, a cluster named Stock 8 in the constellation of Auriga would be an ideal candidate for this analysis as it is comprised of approximately 50 % RR Lyrae variable stars and 50 % main sequence stars. By using a collection of stars as well as a collection of calibrations stars allows for averaged values that more accurately follow the theoretical models of zero point (5) and extinction due to the atmosphere due to air mass (4). An advantage of this is the resultant model is more likely to be applicable to the entire class of stars.

To construct a model a graphical based programming language such as Python or C would be required and at each stage in the stars variation a Temperature, opacity, gravitational acceleration and density would be required to determine the next stage in the time evolution, this could be done by solving a differential equation derived by starting from the polytropic index [9], continuity equation and luminosity emitted from a black body to explain the change in $P(r, T, m, \kappa)$ (where P is the pressure as a function on radius, temperature, mass and opacity) within a shell of the convection

layer of a star, (the derivation of which is complicated and beyond the scope of this report, however, could be done as in a more extended analysis).

7 Conclusion

This report proposes the construction of a stellar model for a short period intrinsic variable star based entirely on optical astronomical data of multiple spectral bands from a cluster of sources, and shows how the analysis can be completed for a single star.

By constructing light curves through the analysis of optical data and determination of the variation in temperature of the star it would be possible to derive a set of differential equations to predict how the internal structure of the star must change with time as it oscillates. This model may help in the understanding of how stars on the main sequence evolve into these short period variable stars and how variable stars evolve off of the strip of instability, furthering our understanding of stellar evolution and the universe.

This concept requires further work to accurately construct models based on empirical data and to reduce the errors when doing so, this is currently planned to be carried out over the summer and this report will be used as a foundation.

References

[1] R. Hollow.

[2] M. Templeton, "Delta Scuti and the Delta Scuti variables."

[3] P. Wils, K. Panagiotopoulos, J. van Wassenhove, A. Ayiomamitis, F. Nieuwenhout, C. W. Robertson, M. Vanleenhove, F.-J. Hambsch, H. Hautecler, R. D. Pickard, A. Baillien, B. Staels, S. Kleidis, P. Lampens, and P. van Cauteren, "Photometry of High-Amplitude Delta Scuti Stars," *Information Bulletin on Variable Stars*, vol. 6015, p. 1, Mar. 2012.

[4] M. S. Bessell, "UBVRI passbands.," , vol. 102, pp. 1181–1199, Oct. 1990.

[5] M. Fukugita, N. Yasuda, M. Doi, J. E. Gunn, and D. G. York, "Characterization of sloan digital sky survey stellar photometry," *The Astronomical Journal*, vol. 141, p. 47, Jan. 2011.

[6] J. A. Guzik, C. J. Fontes, and C. Fryer, "Opacity effects on pulsations of main-sequence a-type stars," *Atoms*, vol. 6, no. 2, 2018.

[7] Lefever, K., Puls, J., and Aerts, C., "Statistical properties of a sample of periodically variable b-type supergiants* - evidence for opacity-driven gravity-mode oscillations," *AA*, vol. 463, no. 3, pp. 1093–1109, 2007.

[8] S. Wang, X. Chen, J. Zhang, and L. Deng, "Double-mode rr lyrae star – robust distance and metallicity indicators," 2023.

[9] S. Turck-Chièze, M. L. Pennec, J. E. Ducret, J. Colgan, D. P. Kilcrease, C. J. Fontes, N. Magee, F. Gilleron, and J. C. Pain, "Detailed opacity comparison for an improved stellar modeling of the envelopes of massive stars," *The Astrophysical Journal*, vol. 823, p. 78, may 2016.

[10] O. F. et. al, " The VizieR database of astronomical catalogues ."

[11] E. Poretti, "VizieR Online Data Catalog: Monoperiodic pulsating stars in the OGLE database (Poretti, 2001)." VizieR On-line Data Catalog: J/A+A/371/986. Originally published in: 2001A&A...371..986P, Mar. 2001.

[12] Stellarium contributors, "Stellarium v23.4 astronomy software," 2023.

[13] Bonnarel, F., Fernique, P., Bienaymé, O., Egret, D., Genova, F., Louys, M., Ochsenbein, F., Wenger, M., and Bartlett, J. G., "The aladin interactive sky atlas - a reference tool for identification of astronomical sources," *Astron. Astrophys. Suppl. Ser.*, vol. 143, no. 1, pp. 33–40, 2000.

[14] M. Fukugita, T. Ichikawa, J. E. Gunn, M. Doi, K. Shimasaku, and D. P. Schneider, "The Sloan Digital Sky Survey Photometric System," , vol. 111, p. 1748, Apr. 1996.

[15] D. Lang, D. W. Hogg, K. Mierle, M. Blanton, and S. Roweis, "Astrometry.net: Blind Astrometric Calibration of Arbitrary Astronomical Images," , vol. 139, pp. 1782–1800, May 2010.

[16] S. Littlefair, "Photometric systems."

[17] L. Casagrande and D. A. VandenBerg, "Synthetic stellar photometry – i. general considerations and new transformations for broad-band systems," *Monthly Notices of the Royal Astronomical Society*, vol. 444, p. 392–419, Aug. 2014.

[18] Carretta, E., Bragaglia, A., Gratton, R. G., Recio-Blanco, A., Lucatello, S., D'Orazi, V., and Cassisi, S., "Properties of stellar generations in globular clusters and relations with global parameters ***," *AA*, vol. 516, p. A55, 2010.

[19] Faustini, F., Molinari, S., Testi, L., and Brand, J., "Properties of stellar clusters around high-mass young stars ***," *AA*, vol. 503, no. 3, pp. 801–816, 2009.

Statement of work

During this lab I have written all the code myself except for my calculation of the zero point for calibrating the magnitude, this was written by student 1 as I was running into issues in the calibration stars I was using. Initial concepts for code were supplied by demonstrators but this code has been heavily modified by the final version. The demonstrators were great help in understanding concepts especially those referring to errors, the zero point and how to observe stars in real world applications, some equations used for errors were derived by demonstrators but the application of these errors was completed by myself.

The data used has been acquired by Paul Kent some of which in association with student (by giving celestial coordinates they wanted observed) and some by Paul himself, the main data set used here (NSVS7293918) I believe was captured by Paul with no input from the group.

Key concepts were discussed between student 1 and myself outside of the lab time but these were mostly brainstorming sessions such as what values could be derived from light curves. The idea to construct a stellar model was my own and has been discussed with demonstrators and student 1 who advised not doing a full model due to the time limit of this lab. Further work is planned on the stellar model in association with Paul Kent and student 1 using this report as a foundation.